

# Synthesis, Electronic Spectra, and Crystal Structural Properties of Fluorinated [3<sub>3</sub>](1,3,5)cyclophanes<sup>†</sup>

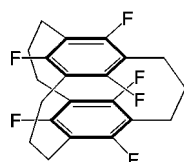
Toru Koga,<sup>‡,§</sup> Mikio Yasutake,<sup>‡,§</sup> and Teruo Shinmyozu<sup>\*,†</sup>

*Institute for Fundamental Research of Organic Chemistry (IFOC) and Department of Chemistry, Graduate School of Science, Kyushu University, Hakozaki, Fukuoka 812-8581, Japan*

shinmyo@ms.ifoc.kyushu-u.ac.jp

Received January 4, 2001

## ABSTRACT

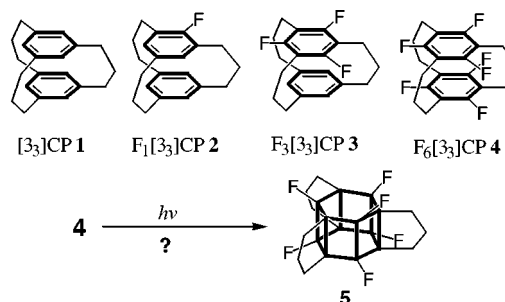


Trifluoro- and hexafluoro[3<sub>3</sub>](1,3,5)cyclophanes **3** and **4** were synthesized with TosMIC coupling as a key reaction. The  $\pi$ – $\pi^*$  absorption bands show blue shifts as the number of fluorine atoms is increased. In the crystalline state, characteristic stacking with the fluorinated benzene rings facing each other is observed in both cases.

Despite much effort, hexaprismane and its derivatives have so far eluded synthesis, mainly due to the lack of appropriate synthetic routes and their expected highly strained nature. In our approach to construct the hexaprismane skeleton by irradiating multibridged [3<sub>n</sub>]cyclophanes ( $n = 3$ –6)<sup>1</sup> with completely stacked benzene rings, we have reported that irradiation of [3<sub>3</sub>](1,3,5)cyclophane ([3<sub>3</sub>]CP) **1**<sup>2</sup> as well as [3<sub>4</sub>](1,2,3,5)-<sup>3</sup> and (1,2,4,5)CP's<sup>4</sup> afforded novel polycyclic cage compounds. These may have been formed by protonation of hexaprismane derivatives, followed by rearrange-

ment of the resultant carbocations and trapping of the stable cations by nucleophiles present under the reaction conditions. It is well-known that a fluorine atom attached to a carbon–carbon bond strengthens the bond and, hence, highly strained compounds may be stabilized by the introduction of fluorine atoms in place of hydrogen atoms.<sup>5</sup> Therefore, the stabilization and lowering of the chemical reactivity of the hexaprismane derivative **5** may lead to its isolation (Scheme 1).

**Scheme 1.** Expected Photochemical Conversion of **4** to F<sub>6</sub>-Propella[3<sub>3</sub>]prismane **5**



<sup>†</sup> Multibridged [3<sub>n</sub>]cyclophanes. 14.

<sup>‡</sup> Institute for Fundamental Research of Organic Chemistry.

<sup>§</sup> Department of Chemistry.

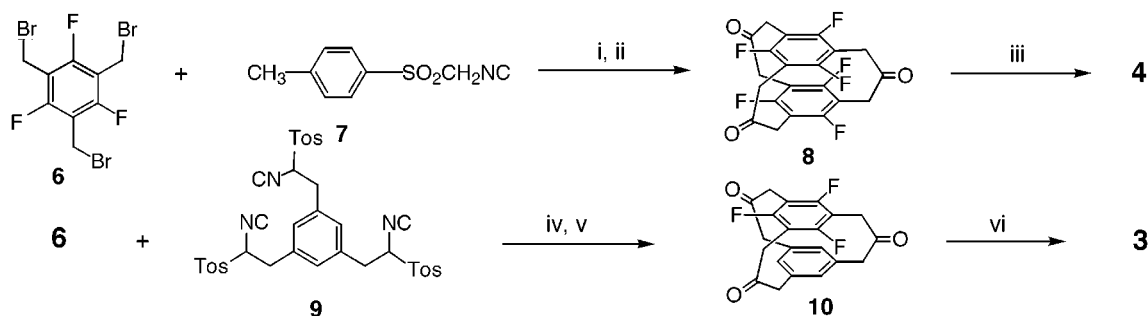
(1) (a) Sakamoto, Y.; Miyoshi, N.; Shinmyozu, T. *Angew. Chem., Int. Ed. Engl.* **1996**, *35*, 549. (b) Sakamoto, Y.; Miyoshi, N.; Hirakida, M.; Kusumoto, S.; Kawase, H.; Rudzinski, J. M.; Shinmyozu, T. *J. Am. Chem. Soc.* **1996**, *118*, 12267. (c) Sakamoto, Y.; Shinmyozu, T. *Recent Res. Devel. Pure Appl. Chem.* **1998**, *2*, 371. (d) Sentou, M.; Satou, T.; Yasutake, M.; Lim, C.; Sakamoto, Y.; Itoh, T.; Shinmyozu, T. *Eur. J. Org. Chem.* **1999**, 1223.

(2) (a) Sakamoto, Y.; Kumagai, T.; Matohara, K.; Lim, C.; Shinmyozu, T. *Tetrahedron Lett.* **1999**, *40*, 919. (b) Matohara, K.; Lim, C.; Yasutake, M.; Nogita, R.; Koga, T.; Sakamoto, Y.; Shinmyozu, T. *Tetrahedron Lett.* **2000**, *41*, 6803.

(3) Lim, C.; Yasutake, M.; Shinmyozu, T. *Tetrahedron Lett.* **1999**, *40*, 6781.

(4) Lim, C.; Yasutake, M.; Shinmyozu, T. *Angew. Chem., Int. Ed.* **2000**, *39*, 578.

**Scheme 2.** Synthetic Routes to the F<sub>6</sub>- and F<sub>3</sub>[3<sub>3</sub>]CP's **4** and **3**<sup>a</sup>



<sup>a</sup> (i) NaOH, *n*-Bu<sub>4</sub>NI, CH<sub>2</sub>Cl<sub>2</sub>–H<sub>2</sub>O, reflux, 10 h; (ii) concentrated HCl, CH<sub>2</sub>Cl<sub>2</sub>, room temperature (7%); (iii) KOH, H<sub>2</sub>NNH<sub>2</sub>·H<sub>2</sub>O, diethylene glycol (12%); (iv) NaH, DMF, room temperature, overnight; (v) concentrated HCl, CH<sub>2</sub>Cl<sub>2</sub>, room temperature (10%); (vi) KOH, H<sub>2</sub>NNH<sub>2</sub>·H<sub>2</sub>O, diethylene glycol (62%).

We would like to report here the successful synthesis of the tri- and hexafluoro[3<sub>3</sub>]CP's **3** and **4** as precursors to the photoreaction and their interesting crystal structural properties. Previously, we reported the first crystal structure of [3<sub>6</sub>]- (1,2,3,4,5,6)CP as a TCNQ–F<sub>4</sub> complex<sup>6</sup> and the relationship between the crystal structural properties and conductivities of the charge transfer (CT) complexes of [3<sub>3</sub>]CP **1** and [3<sub>6</sub>]- (1,2,3,4,5,6)CP with TCNQ and TCNQ–F<sub>4</sub>.<sup>7</sup>

F<sub>6</sub>[3<sub>3</sub>]CP **4** was synthesized by TosMIC coupling<sup>8</sup> between 1,3,5-tris(bromomethyl)-2,4,6-trifluorobenzene **6**<sup>9</sup> and TosMIC **7**<sup>10</sup> under phase-transfer conditions (Scheme 2), followed by acid hydrolysis (7%) and the reduction of the resultant F<sub>6</sub>-ketone **8** (12%).<sup>11</sup> Similarly, coupling of **6** with the TosMIC adduct **9** in the presence of NaH in DMF<sup>12</sup> and subsequent acid hydrolysis gave the ketone **10** (10%). Reduction of the carbonyl groups of **10** afforded F<sub>3</sub>[3<sub>3</sub>]CP **3** (62%).<sup>13</sup> The

yields of the TosMIC coupling were low, but our synthetic routes provided straightforward and short-step approaches to the fluorinated [3<sub>3</sub>]CP's.

The <sup>1</sup>H NMR spectrum of **3** shows the aromatic proton signal at 6.82 ppm as a singlet. In the <sup>19</sup>F NMR spectra, the fluorine signals of **3** and **4** appear as singlets at 45.8 and 46.3 ppm from C<sub>6</sub>F<sub>6</sub>, respectively. These NMR data are in good agreement with the expected structures and suggest that the trimethylene bridges are mobile at ambient temperatures.<sup>14</sup>

Figure 1 shows the electronic spectra of a series of F<sub>1</sub>-, F<sub>3</sub>-, and F<sub>6</sub>[3<sub>3</sub>]CPs **2**, **3**, and **4** along with the parent **1** as a

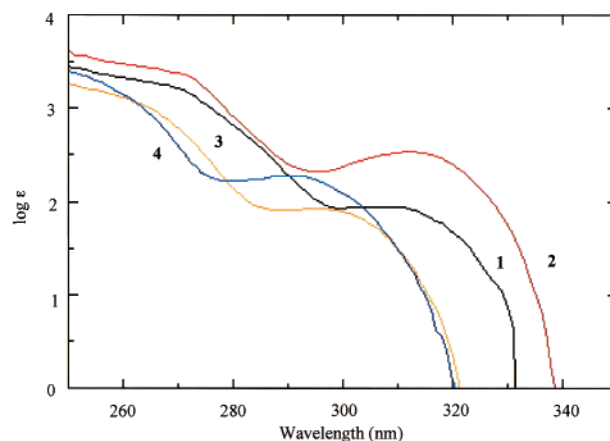


**Figure 1.** Electronic spectra of [3<sub>3</sub>]CP **1**, F<sub>1</sub>[3<sub>3</sub>]Cp **2**, F<sub>3</sub>[3<sub>3</sub>]Cp **3**, and F<sub>6</sub>[3<sub>3</sub>]CP **4** in CHCl<sub>3</sub>.

reference in CHCl<sub>3</sub>. Although the longest wavelength  $\pi$ – $\pi^*$  band ( $\lambda_{\max}$ ) of **2** (313 nm,  $\epsilon$  337)<sup>15</sup> shows a slight red shift compared with that of **1** (308 nm,  $\epsilon$  88), the band shows a

(5) (a) Camggi, C.; Gozzo, F.; Ceviddali, G. B. *J. Chem. Soc., Chem. Commun.* **1966**, 313. (b) Briond, M. G.; Hszelclins, R. N. *J. Chem. Soc., Perkin Trans. 1* **1975**, 2005.

(6) Yasutake, M.; Sakamoto, Y.; Onaka, S.; Sako, K.; Tatemitsu, H.; Shinmyozu, T. *Tetrahedron Lett.* **2000**, 41, 7933.

(7) Yasutake, M.; Koga, T.; Sakamoto, Y.; Komatsu, S.; Sako, K.; Tatemitsu, H.; Aso, Y.; Inoue, S.; Shinmyozu, T. Submitted.

(8) (a) Kurosawa, K.; Suenaga, M.; Inazu, T.; Yoshino, T. *Tetrahedron Lett.* **1982**, 23, 5335. (b) Shinmyozu, T.; Hirai, Y.; Inazu, T. *J. Org. Chem.* **1986**, 51, 1551. (c) Sasaki, H.; Kitagawa, T. *Chem. Pharm. Bull.* **1983**, 31, 2868.

(9) An important intermediate, **6**, was prepared starting from 1,3,5-trifluorobenzene by the chloromethylation with ClCH<sub>2</sub>OCH<sub>3</sub> in the presence of AlCl<sub>3</sub> in refluxing CS<sub>2</sub> (80%), followed by the halogen exchange of the resultant 1,3,5-tris(chloromethyl)-2,4,6-trifluorobenzene with NaBr–EtBr in DMF (78%). **6**: colorless crystals (CH<sub>2</sub>Cl<sub>2</sub>); <sup>1</sup>H NMR (CDCl<sub>3</sub>)  $\delta$  4.48 (s, 6H, CH<sub>2</sub>Br); <sup>19</sup>F NMR (CDCl<sub>3</sub>, C<sub>6</sub>F<sub>6</sub>)  $\delta$  47.6 (s); FAB-MS *m/z* 408.9 [M<sup>+</sup>]. Anal. Calcd for C<sub>9</sub>H<sub>6</sub>Br<sub>3</sub>F<sub>3</sub>: C, 26.31; H, 1.47. Found: C, 26.50; H, 1.46.

(10) (a) Hoogenboom, B. E.; Oldenzel, O. H.; van Leusen, A. M. *Organic Syntheses*; Wiley: New York, 1988; Collect. Vol. 6, p 987. (b) Possel, O.; van Leusen, A. M. *Tetrahedron Lett.* **1977**, 4229.

(11) **Selected spectroscopic data and elemental analysis for 4**: colorless crystals (hexane). This compound shows complex phase transition phenomenon. The details will be reported in a full paper on this work. <sup>1</sup>H NMR (CDCl<sub>3</sub>)  $\delta$  2.26 (m, 6H), 2.78–2.83 (m, 12H); <sup>19</sup>F NMR (CDCl<sub>3</sub>, C<sub>6</sub>F<sub>6</sub>)  $\delta$  46.3 (s, 6F); FAB-MS *m/z* 384.1 [M<sup>+</sup>]. Anal. Calcd for C<sub>21</sub>H<sub>18</sub>F<sub>6</sub>: C, 65.62; H, 4.72. Found: C, 65.90; H, 4.98.

(12) Breitenbach, J.; Vögtle, F. *Synthesis* **1992**, 41.

(13) **Selected spectroscopic data and elemental analysis for 3**: colorless crystals (hexane); mp 109.5–111 °C; <sup>1</sup>H NMR (CDCl<sub>3</sub>)  $\delta$  2.16 (m, 6H), 2.65–2.74 (m, 12H), 6.82 (s, 3H); <sup>19</sup>F NMR (CDCl<sub>3</sub>, C<sub>6</sub>F<sub>6</sub>)  $\delta$  45.8 (s, 3F); FAB-MS *m/z* 330.2 [M<sup>+</sup>]. Anal. Calcd for C<sub>21</sub>H<sub>21</sub>F<sub>3</sub>·0.25H<sub>2</sub>O: C, 75.37; H, 6.48. Found: C, 75.30; H, 6.52.

(14) Meno, T.; Sako, K.; Suenaga, M.; Mouri, M.; Takemura, H.; Shinmyozu, T.; Inazu, T. *Can. J. Chem.* **1990**, 68, 440–445.

(15) Synthesis and characterization of F<sub>1</sub>[3<sub>3</sub>]CP **2** will be reported in a full paper on this work.

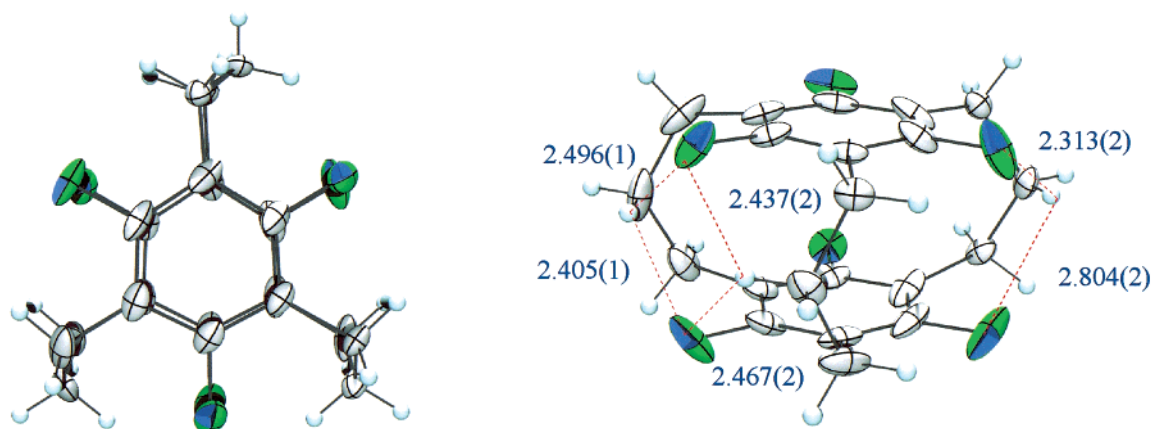


**Figure 2.** Top and side views of  $F_6[3_3]CP$  **4**.

gradual blue shift as the number of fluorine atoms increases: **3** 296 nm ( $\epsilon$  85); **4** 291 nm ( $\epsilon$  188). In principle, the HOMO–LUMO gap estimated by ab initio MO calculations (HF/6-31G) [11.03 (**1**), 11.16 (**2**), 11.19 (**3**), and 11.52 eV (**4**)] supports the phenomenon. This characteristic blue shift is explained in terms of significant lowering of the HOMO level and modest lowering of the LUMO level as the number of fluorine atoms increases. However, the anomalous behavior of **2** cannot be explained at this stage.

The ORTEP drawings and crystal packing diagrams of **3** and **4** at  $-180^\circ\text{C}$  are shown in Figures 3 and 2 as well as Figures 4 and 5, respectively.<sup>16</sup> Two molecules (A and B) of **3** are stacked with fluorinated benzene rings facing each other (Figure 4), whereas the neighboring molecule (C) is in a perpendicular orientation to the nonfluorinated face of the benzene ring of molecule (B); this arrangement is generally observed in the crystal packing of  $[3_n]$ cyclophanes.<sup>1d,6</sup> Similarly, molecules of **4** are stacked with fluorinated

benzene rings facing each other and form an infinite column (Figure 5), while formation of such a column is not observed for **3**. The intermolecular transannular distance between the two benzene rings of **4** (3.309 Å) is much shorter than that in **3** (3.518 Å), and this indicates that the interaction between two fluorinated benzene rings in **4** is stronger than in **3**.

Both **3** and **4** are in  $C_s$  conformations rather than an alternative  $C_{3h}$  symmetry in the crystals at  $-180^\circ\text{C}$ . In the parent **1**, the  $C_s$  conformer is more stable than the  $C_{3h}$  one by 0.4 kcal/mol in  $\text{CD}_2\text{Cl}_2$  at  $-70^\circ\text{C}$ , and the energy barrier to the bridge inversion is 12.4 kcal/mol.<sup>14</sup> The intramolecular transannular distances between the two benzene rings of **4** are 3.028(3)–3.059(2) Å for the bridged carbon atoms and 3.070(2)–3.157(3) Å for the unbridged carbon atoms, and these are slightly shorter than the corresponding distances of **3** [3.036(2)–3.082(2) Å and 3.066(2)–3.162(2) Å]. Quite interestingly, some short H–F contacts between a methylene proton of the central carbon atom of the bridge and a fluorine

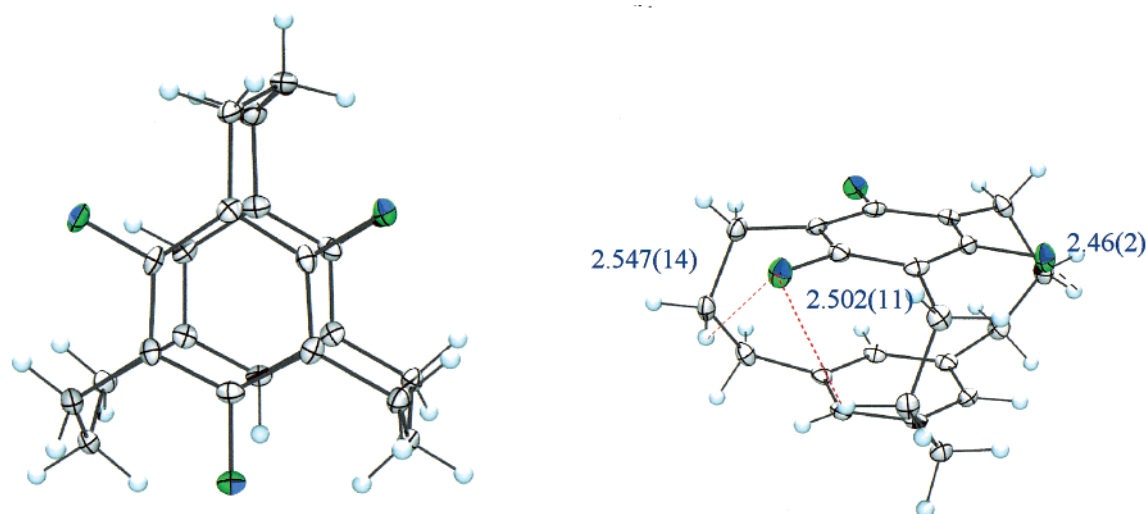


**Figure 3.** Top and side views of  $F_3[3_3]CP$  **3**.

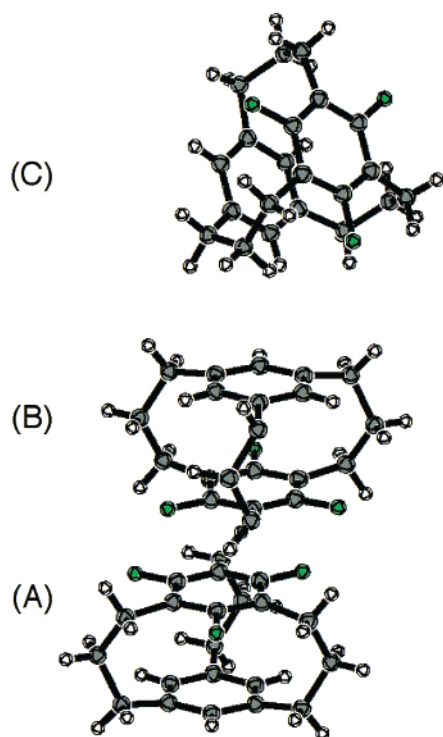


Figure 4. Crystal packing diagram of  $F_3[3_3]CP$  3.

atom attached to the benzene ring are observed in the crystal structure of **4** (H–F 2.313(2), 2.405(1) Å). These H–F values are smaller than the sum of the van der Waals radii of a hydrogen atom and a fluorine atom (2.43 Å), and these data suggest the presence of weak H–F bonds reminiscent of the H–N bonds of lone pair electrons of the pyridyl nitrogen and neighboring protons of 2,11-diaza[3<sub>2</sub>](2,6)-pyridinophane, reported previously.<sup>17</sup> Slightly shorter intramolecular transannular distances between the two benzene rings in **4** than in **3** may be attributed to the stronger H–F interaction in **4** than in **3**.

In conclusion,  $F_3$ - and  $F_6[3_3]CP$ 's **3** and **4** were synthesized. The longest  $\pi$ – $\pi^*$  absorption band shows a blue shift

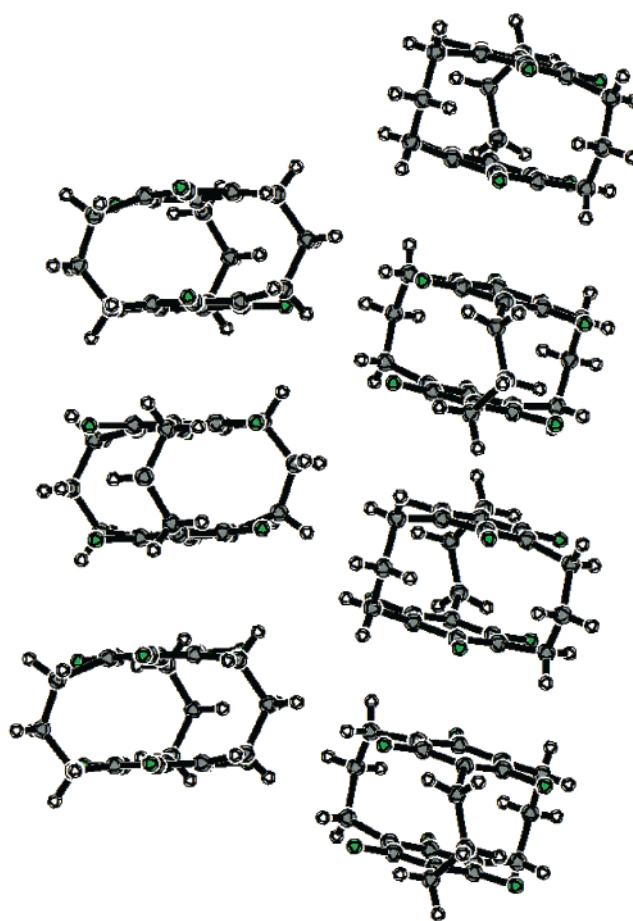


Figure 5. Crystal packing diagram of  $F_6[3_3]CP$  4.

as the number of fluorine atoms is increased. In the crystalline state, both molecules exist in  $C_s$  conformations, molecules are stacked with the fluorinated benzene rings facing each other, and the repeated stacking forms a column in **4**. This phenomenon is a characteristic feature of the fluorinated derivatives because the neighboring two molecules are perpendicular in all nonfluorinated  $[3_n]CP$ 's ( $n = 3$ –6). The H–F hydrogen bond-like interaction is more significant in **4** than in **3**.<sup>18</sup> Photochemical reactions of **3** and **4** are in progress and will be reported elsewhere.

**Acknowledgment.** We gratefully acknowledge financial support from a Grant-in-Aid for the Priority Area (A) of Creation of Delocalized Electronic Systems (no. 12020241) from the Ministry of Education, Science, Sports and Culture, Japan.

OL010003W

(16) The cyclophanes **3** and **4** were recrystallized from  $CH_2Cl_2$ –hexane (1:1 v/v). X-ray crystal data **3** ( $C_{21}H_{18}F_3$ ): Rigaku R-Axis-RAPID diffractometer, Mo  $K\alpha$  ( $\lambda = 0.71070$  Å), crystal dimensions  $0.40 \times 0.15 \times 0.40$  mm<sup>3</sup> (colorless prism),  $a = 14.0736(5)$ ,  $b = 9.3114(4)$ , and  $c = 13.4596(5)$  Å,  $\beta = 61.492(2)^\circ$ , monoclinic space group  $P2_1/a$  (No. 14),  $T = -180$  °C,  $Z = 4.0$ ,  $\mu_{Mo} = 1.05$  cm<sup>−1</sup>,  $M_r = 330.39$ ,  $V = 1550.0(1)$  Å<sup>3</sup>, anode power 50 kV  $\times$  32 mA,  $\rho_{calcd} = 1.416$  g/cm<sup>3</sup>,  $2\theta_{max} = 55.0^\circ$ ,  $F(000) = 696.00$ . A total of 6784 reflections were measured, 4095 observed ( $I > 3.00\sigma(I)$ ), number of parameters 302. The structure was solved by a direct method and was refined on  $Sir92$ .<sup>19</sup> Data were corrected for Lorentz polarizations. The data/parameter ratio was 13.56.  $R = 0.0035$ ,  $R_w = 0.042$ , GOF = 1.13, max/min residual density  $+0.23/-0.21$  e Å<sup>−3</sup>. X-ray crystal data for **4** ( $C_{21}H_{18}F_6$ ): Rigaku R-Axis-RAPID diffractometer, Mo  $K\alpha$  ( $\lambda = 0.71070$  Å), crystal dimensions  $0.50 \times 0.50 \times 0.50$  mm<sup>3</sup> (colorless prism),  $a = 9.6178(4)$ ,  $b = 14.2330(6)$ , and  $c = 12.4812(4)$  Å,  $\beta = 108.725(2)^\circ$ , monoclinic space group  $P2_1/a$  (No. 14),  $T = -180$  °C,  $Z = 4.0$ ,  $\mu_{Mo} = 1.39$  cm<sup>−1</sup>,  $M_r = 384.36$ ,  $V = 1618.1(1)$  Å<sup>3</sup>, anode power 50 kV  $\times$  32 mA,  $\rho_{calcd} = 1.578$  g/cm<sup>3</sup>,  $2\theta_{max} = 55.0^\circ$ ,  $F(000) = 792.00$ . A total of 3701 reflections were measured, 2739 observed ( $I > 3.00\sigma(I)$ ), number of parameters 272. The structure was solved by a direct method and was refined on SAPI91.<sup>20</sup> Data were corrected for Lorentz polarizations. The data/parameter ratio was 10.07.  $R = 0.0059$ ,  $R_w = 0.104$ , GOF = 1.60, max/min residual density  $+0.50/-0.67$  e Å<sup>−3</sup>.

(17) (a) Wen, G.; Matsuda-Sentou, W.; Sameshima, K.; Yasutake, M.; Noda, D.; Lim, C.; Satou, T.; Takemura, H.; Sako, K.; Tatemitsu, H.; Inazu, T.; Shinmyozu, T. Submitted. (b) Sako, K.; Tatemitsu, H.; Onaka, S.; Takemura, H.; Osada, S.; Wen, G.; Rudzinski, J. M.; Shinmyozu, T. *Liebigs Ann.* **1996**, 1645.

(18) Takemura, H.; Nakashima, S.; Kon, N.; Yasutake, M.; Shinmyozu, T.; Inazu, T. Submitted.

(19) Altomare, A.; Burla, M. C.; Camalli, M.; Cascarano, M.; Giacovazzo, C.; Guagliardi, A.; Polidori, G. *J. Appl. Crystallogr.* **1994**, 27, 435.

(20) Fan Hai-Fu, Structure Analysis Program with Intelligent Control, Rigaku Corporation, Tokyo, Japan.